

## Supplemental Figure Legends

### Supplemental Figure 1

Determination of therapeutic time window of anti-HMGB1 mAb treatment in rat TBI.

(A) After fluid percussion injury, the rats received intravenous injection of anti-HMGB1 (1mg/kg) or control mAb at 5 minutes, 3 hours or 6 hours. The rotarod test was performed 6 hours after injury. Results are expressed as mean  $\pm$  SEM of 5 or 6 rats. #P < 0.05 compared with injured control rats treated with control mAb. (B)

The rats received intravenous injection of anti-HMGB1 (1mg/kg) or control mAb at 3 hours or 6 hours. The permeability of brain capillary vessels was examined by intravenously injecting Evans blue (40 mg/kg) at 6 hours after injury and then measuring the leakage of Evans-blue-albumin into brain parenchyma 3 hours after Evans blue injection. Representative three individuals are shown. (C) Results are expressed as % reduction of Evans blue content by anti-HMGB1 treatment at different time points. The results are the mean  $\pm$  SEM of 5-7 rats. #P < 0.05 compared with injured control rats treated with control mAb.

### Supplemental Figure 2

Long-term beneficial effects of anti-HMGB1 mAb on impairment of motor activity and neuronal death in TBI rats. (A) After fluid percussion injury, the rats received intravenous injection of anti-HMGB1 (1mg/kg) or control mAb at 5 minutes and 6 hours. Then the same dose of mAb was administered daily. The rotarod test was performed at 7 and 14 days after injury. Results are expressed as mean  $\pm$  SEM of 5

rats. #P < 0.05 compared with injured control rats treated with control mAb. (B) Seven days after injury, the rat brain was fixed with transcardial perfusion with formalin and the neuronal death in the cerebral cortex (5 mm rostral to the injured center) and hippocampal CA1 area (dorsal hippocampus below the injured center) was evaluated by Nissl staining. The representative pictures were shown. (C) The percentage of pyknotic cells was counted in three fields in both areas in each rat. Results are expressed as mean  $\pm$  SEM of 5 rats. #P < 0.05 compared with injured control rats treated with control mAb.

### Supplemental Figure 3

Dose-effect relationship for anti-HMGB1 mAb treatment in rat TBI.

(A) After fluid percussion injury, the rats received intravenous injection of anti-HMGB1mAb (0.33, 0.67 or 1mg/kg) at 5 minutes. The rotarod test was performed 6 hours after injury. Results are expressed as mean  $\pm$  SEM of 5 or 6 rats. #P < 0.05 compared with injured control rats treated with control mAb.

(B) The rats received intravenous injection of anti-HMGB1 mAb (0.33, 0.67 or 1mg/kg) at 5 min after injury. The permeability of brain capillary vessels was examined by intravenously injecting Evans blue (40 mg/kg) at 6 hours after injury and then measuring the leakage of Evans-blue-albumin into brain parenchyma 3 hours after Evans blue injection. Representative three individuals are shown. (C) Results are expressed as % reduction of Evans blue content by anti-HMGB1 treatment at different doses. The results are the mean  $\pm$  SEM of 5-7 rats. #P < 0.05 compared with injured control rats treated with control mAb.

# Stroke

American Stroke  
Association<sup>SM</sup>

JOURNAL OF THE AMERICAN HEART ASSOCIATION

A Division of American  
Heart Association



## **Anti-high Mobility Group Box-1 Monoclonal Antibody Protects the Blood–Brain Barrier From Ischemia-Induced Disruption in Rats**

Jiyong Zhang, Hideo K. Takahashi, Keyue Liu, Hidenori Wake, Rui Liu, Tomoko Maruo, Isao Date, Tadashi Yoshino, Aiji Ohtsuka, Shuji Mori and Masahiro Nishibori

*Stroke* 2011, 42:1420-1428: originally published online April 7, 2011

doi: 10.1161/STROKEAHA.110.598334

Stroke is published by the American Heart Association, 7272 Greenville Avenue, Dallas, TX 75214  
Copyright © 2011 American Heart Association. All rights reserved. Print ISSN: 0039-2499. Online  
ISSN: 1524-4628

The online version of this article, along with updated information and services, is  
located on the World Wide Web at:

<http://stroke.ahajournals.org/content/42/5/1420>

Data Supplement (unedited) at:

<http://stroke.ahajournals.org/content/suppl/2011/04/27/STROKEAHA.110.598334.DC1.html>

Subscriptions: Information about subscribing to *Stroke* is online at  
<http://stroke.ahajournals.org//subscriptions/>

Permissions: Permissions & Rights Desk, Lippincott Williams & Wilkins, a division of Wolters  
Kluwer Health, 351 West Camden Street, Baltimore, MD 21202-2436. Phone: 410-528-4050. Fax:  
410-528-8550. E-mail:  
[journalpermissions@lww.com](mailto:journalpermissions@lww.com)

Reprints: Information about reprints can be found online at  
<http://www.lww.com/reprints>

# Anti-high Mobility Group Box-1 Monoclonal Antibody Protects the Blood–Brain Barrier From Ischemia-Induced Disruption in Rats

Jiyong Zhang, PhD\*; Hideo K. Takahashi, MD, PhD\*; Keyue Liu, MD, PhD; Hidenori Wake, PhD; Rui Liu, PhD; Tomoko Maruo, MD; Isao Date, MD, PhD; Tadashi Yoshino, MD, PhD; Aiji Ohtsuka, MD, PhD; Shuji Mori, PhD; Masahiro Nishibori, MD, PhD

**Background and Purpose**—High mobility group box-1 (HMGB1) exhibits inflammatory cytokine-like activity in the extracellular space. We previously demonstrated that intravenous injection of anti-HMGB1 monoclonal antibody (mAb) remarkably ameliorated brain infarction induced by middle cerebral artery occlusion in rats. In the present study, we focused on the protective effects of the mAb on the marked translocation of HMGB1 in the brain, the disruption of the blood–brain barrier (BBB), and the resultant brain edema.

**Methods**—Middle cerebral artery occlusion in the rat was used as the ischemia model. Rats were treated with anti-HMGB1 mAb or control IgG intravenously. BBB permeability was measured by MRI. Ultrastructure of the BBB unit was observed by transmission electron microscope. The in vitro BBB system was used to study the direct effects of HMGB1 in BBB components.

**Results**—HMGB1 was time-dependently translocated and released from neurons in the ischemic rat brain. The mAb reduced the edematous area on T2-weighted MRI. Transmission electron microscope observation revealed that the mAb strongly inhibited astrocyte end feet swelling, the end feet detachment from the basement membrane, and the opening of the tight junction between endothelial cells. In the in vitro reconstituted BBB system, recombinant HMGB1 increased the permeability of the BBB with morphological changes in endothelial cells and pericytes, which were inhibited by the mAb. Moreover, the anti-HMGB1 mAb facilitated the clearance of serum HMGB1.

**Conclusions**—These results indicated that the anti-HMGB1 mAb could be an effective therapy for brain ischemia by inhibiting the development of brain edema through the protection of the BBB and the efficient clearance of circulating HMGB1. (*Stroke*. 2011;42:1420-1428.)

**Key Words:** blood–brain barrier ■ brain edema ■ electron microscopy ■ HMGB1 ■ MRI

Disruption of the blood–brain barrier (BBB) is a critical event in the formation of brain edema during the early phase of ischemic brain injury. BBB permeability can be increased by several factors, including cytokines, vascular endothelial growth factor, and nitric oxide.<sup>1,2</sup> Among these factors, cytokines have been widely described as vital players such as interleukin-1 $\beta$  and tumor necrosis factor- $\alpha$ .<sup>3,4</sup> High mobility group box-1 (HMGB1) is a ubiquitous and abundant nonhistone DNA-binding protein, which is newly defined as a cytokine that can be passively released from necrotic cells or positively released from immune activated cells under the stimulation of inflammatory signals, thus inducing inflammatory responses in sepsis, acute lung injury, and rheumatoid arthritis.<sup>5-7</sup> Recently, HMGB1 has received particular atten-

tion with respect to its pathological role in cerebral ischemia. In transient middle cerebral artery occlusion (MCAO) in mice and rats, HMGB1 was found to be translocated into the cytoplasmic compartment from nuclei.<sup>8-11</sup> High levels of serum HMGB1 were observed in patients with stroke compared with healthy control subjects.<sup>12</sup> This early release of HMGB1 into the extracellular space after ischemic injury may contribute to the initial stage of the inflammatory response in the ischemic penumbra.

We previously demonstrated that a neutralizing anti-HMGB1 monoclonal antibody (mAb) remarkably ameliorated brain infarction induced by a 2-hour MCAO in rats and was associated with significantly improved neurological deficits.<sup>9</sup> Although the disruption of the BBB was apparent by the extravasation of

Received August 6, 2010; final revision received November 14, 2010; accepted December 13, 2010.

From the Departments of Pharmacology (J.Z., H.K.T., K.L., H.W., R.L., M.N.), Neurosurgery (T.M., I.D.), Pathology (T.Y.), and Human Morphology (A.O.), Okayama University Graduate School of Medicine, Dentistry, and Pharmacological Sciences, Okayama, Japan; and the Department of Pharmacy (S.M.), Shujitsu University, Okayama, Japan.

The online-only Data Supplement is available at <http://stroke.ahajournals.org/cgi/content/full/STROKEAHA.110.598334/DC1>.

\*J.Z. and H.K.T. contributed equally to this work.

Correspondence to Masahiro Nishibori, MD, PhD, Department of Pharmacology, Okayama University Graduate School of Medicine, Dentistry and Pharmacological Sciences, Okayama 700-8558, Japan. E-mail [mnbori@md.okayama-u.ac.jp](mailto:mnbori@md.okayama-u.ac.jp)

© 2011 American Heart Association, Inc.

*Stroke* is available at <http://stroke.ahajournals.org>

DOI: 10.1161/STROKEAHA.110.598334

Evans blue dye even at 3 hours after reperfusion in the control animals, the anti-HMGB1 mAb efficiently inhibited protein leakage and the activation of matrix metalloproteinase-9, which has been suggested to be an initial factor inducing endothelial tight junction (TJ) degradation in BBB disruption.<sup>13,14</sup> Therefore, we hypothesized that HMGB1 may contribute to BBB disruption during the acute phase of ischemia/reperfusion.

The present study was undertaken to further investigate the mechanism of the HMGB1-neutralizing mAb from the aspect of maintaining the BBB functionally and structurally. First, we analyzed the time course of HMGB1 translocation and release from brain cells into the cerebrospinal fluid and bloodstream. Second, we observed the changes in the structure of BBB using transmission electron microscopy and T2-weighted MRI. Third, we used the *in vitro* BBB system to demonstrate the direct effects of HMGB1 on the components of the BBB. The results strongly indicated that HMGB1 may induce morphological and functional changes in the BBB, whereas the anti-HMGB1 mAb prevented the increase of BBB permeability through the maintenance of its structure and facilitated the clearance of circulating HMGB1.

## Methods

### MCAO Surgical Procedure

All experimental procedures were conducted in accordance with the guidelines of Okayama University for animal experiments and approved by the university's committee on animal experimentation. Male Wistar rats (Charles River Laboratory Japan, Yokohama, Japan), weighing 250 to 300 g, were used for all experiments. MCAO was performed as previously described.<sup>9</sup> Briefly, the rats were anesthetized with 2% halothane in a mixture of 50% N<sub>2</sub>O and 50% O<sub>2</sub>. An 18-mm-long strand of 4.0 nylon thread coated with silicone was inserted into the right internal carotid artery to occlude the origin of the right middle cerebral artery. The thermocouple needle probe was inserted into temporal muscle to maintain the temperature at 37.0±0.1°C with a heating lamp during surgery. Only the rats that showed paralysis of the contralateral limbs after recovery from anesthesia were used for further experiments. Reperfusion was performed at 2 hours after MCAO. As shown in Supplemental Table 1 (<http://stroke.ahajournals.org>), basic physiological parameters, including blood gases, pH, hemoglobin, and glucose, were monitored. The rats were randomly assigned into 2 groups after MCAO operation, and an anti-HMGB1 mAb (#10-22, IgG<sub>2a</sub> subclass, 200 µg/rat) or class-matched control mAb (anti-*Keyhole Limpet* hemocyanin) was administered intravenously immediately and at 6 hours after reperfusion. All quantitative evaluation of animals was performed by investigators blinded to the treatment.

### Immunohistochemistry Staining

Paraffin-embedded brain sections were stained using a mouse anti-HMGB1 mAb (R&D Systems, Inc, Minneapolis, MN) or a rabbit anti-HMGB1 Ab (Abcam plc, Cambridge, UK). For double immunostaining, the sections were incubated with the mouse anti-HMGB1 mAb (R&D Systems, Inc) in combination with anti-microtubule-associated protein 2 Ab (Santa Cruz Biotechnology, Inc, Santa Cruz, CA), anti-gial fibrillary acidic protein Ab (Abcam plc), or anti-ionized calcium-binding adaptor molecule 1 Ab (Wako, Inc, Osaka, Japan). For aquaporin 4 (AQP4) staining, a mouse anti-AQP4 mAb (Abcam plc) was incubated with frozen sections of rat brains as the primary antibody. See details in the Supplemental Methods (<http://stroke.ahajournals.org>).

### Enzyme-Linked Immunosorbent Assay of HMGB1

For HMGB1 determination in serum samples, blood samples (1 mL) were collected through the inferior vena cava under deep anesthesia with an intraperitoneal injection of sodium pentobarbital (50 mg/kg)

followed by centrifugation at 1500 g for 10 minutes. The supernatants were removed to clean Eppendorf tubes and stored at -20°C before use. Cerebrospinal fluid samples were collected from the cistern magna according to the previously reported method.<sup>15</sup> Samples contaminated by blood were excluded. HMGB1 was determined using an HMGB1 enzyme-linked immunosorbent assay kit (Shino-Test Co, Sagami-hara, Japan) according to the manufacturer's protocol.

### Brain Water Content Measurement

Ten rats were allocated to 3 groups: the sham group (n=4), control mAb-injected group (n=8), and anti-HMGB1 mAb-injected group (n=9). All animals except the intact group were subjected to surgery for MCAO. Three hours after reperfusion, the animals were anesthetized deeply with an intraperitoneal injection of sodium pentobarbital (50 mg/kg). The brains were rapidly removed and dissected into 4 regions: the hippocampus, striatum, hypothalamus, and cerebral cortex in each hemisphere. After weighing, the tissues were dried at 80°C for 8 hours. The water content in each region was calculated according to the following equation: % water content=100×(wet weight-dry weight)/wet weight.

### MRI Examination

Rat brain water changes were examined in a 3.0-T horizontal-bore magnet (GE Signa EXCITE 3.0 T; GE Healthcare, Buckinghamshire, UK) at 3, 6, 12, and 24 hours after reperfusion (n=4 per group). MRI parameters were set with TR/TE=5000/115.18 ms, thickness/gap=2/0.2 mm, field of view=100 mm×100 mm, matrix=480×480, number of excitations=1.5. The body temperature was maintained at 37°C by a heating fan. After the optimal adjustment of contrast, hemisphere intensity was examined using National Institutes of Health image J 1.42q software (National Institutes of Health, Bethesda, MD) using the operation "mean gray value." The intensity percentage of the ipsilateral hemisphere against the contralateral hemisphere was calculated, and statistical analysis was performed. During MRI, a series of 4-slice data were obtained.

### Transmission Electron Microscopic Examination

Three hours after reperfusion, MCAO rats were anesthetized with an intraperitoneal injection of sodium pentobarbital (50 mg/kg) and perfused through the left ventricle with 50 mL of saline followed by 100 mL of 4% paraformaldehyde and 2.5% glutaraldehyde in 0.1 mol/L cacodylic acid buffer (pH 7.3). The fixed brain was dehydrated through an ethanol series embedded in epoxy resin and cut into ultrathin sections. The sections were mounted on copper grids, stained in uranyl acetate and citric acid lead, and then observed under a transmission electron microscope (H-7100; Hitachi Ltd, Tokyo, Japan) equipped in the central laboratory of Okayama University. To quantify the astrocyte end feet swelling, National Institutes of Health image J 1.42q software was used to calculate the ratio of the total swollen astrocyte end feet surrounding against the area of the corresponding capillary lumen. Eight rats were analyzed for each group treated with control Ab or anti-HMGB1 mAb. Seven capillaries in each area were evaluated.

### In Vitro BBB Permeability Assay

An *in vitro* BBB kit (RBE-12; PharmaCo-Cell Co Ltd, Sakamoto, Japan) composed of rat brain vascular endothelial cells, pericytes, and astrocytes was used to assess the effects of recombinant human HMGB1 (rHMGB1) and the mAb to the BBB unit according to the instructions of the manufacturer.<sup>16</sup> The endothelial cells were cultured on the bottom of the polyester membrane of the insert well. The pericytes were present below the membrane of the insert well. The astrocytes were cultured on the bottom of the lower chamber. Endotoxin-free rHMGB1 (see details in Supplemental Methods) alone or together with the anti-HMGB1 mAb was added into the lower chamber, which is supposed to be the brain side. Transendothelial electric resistance and leakage of the Evans blue-albumin complex were measured thereafter. F-actin was stained to observe the morphological changes of endothelial cells and pericytes. See detail in Supplemental Methods.

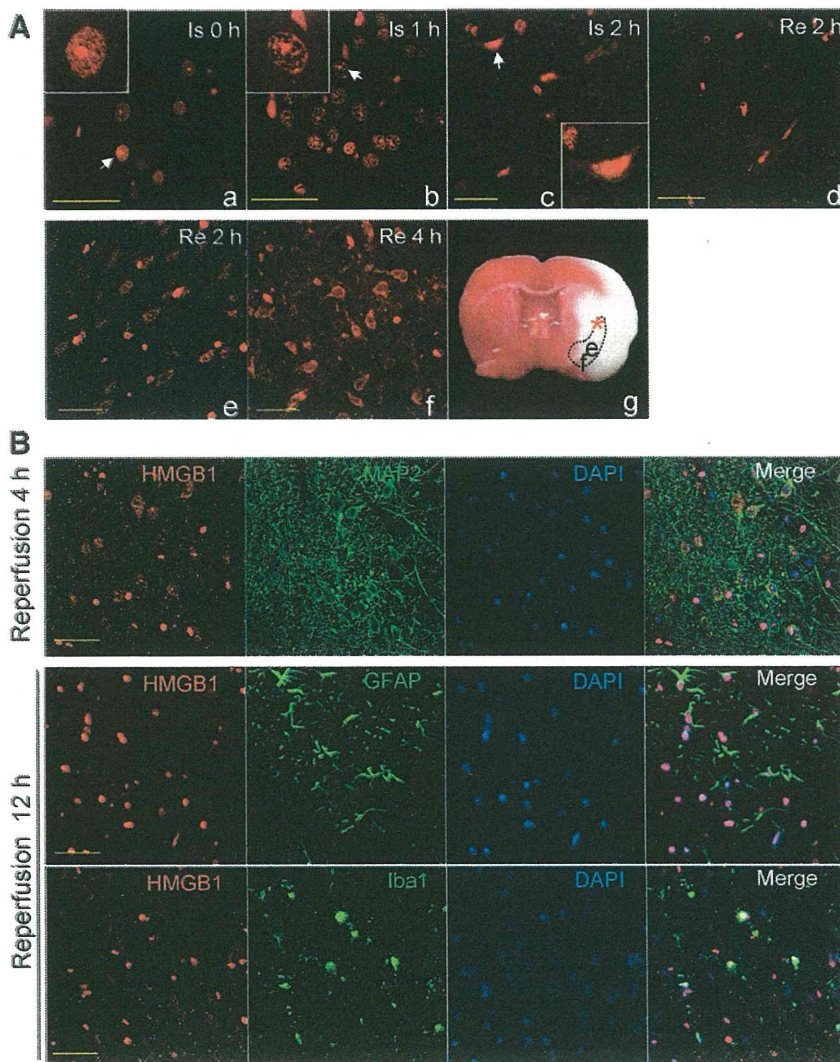


**Figure 1.** Time-dependent translocation of high mobility group box-1 (HMGB1) in neurons of ischemic rat brain. The rat brains were fixed before, during ischemia, and after reperfusion at different time points. **A.** In the normal rat brain (**a**), HMGB1 localized solely in cell nuclei with condensed staining in nucleoli. One hour after ischemia (**b**), HMGB1 was redistributed inside the nuclei forming a “lotus-root like structure” in the ischemic penumbra. Two hours after ischemia (**c**), the cells in the ischemic core of the striatum were reduced in size and HMGB1 was located in the nuclei and cytosol. **d.** Two hours after reperfusion, HMGB1 disappeared in neurons with big nuclei. The typical staining pattern of HMGB1 translocation was observed in the striatum of the ischemic rat brain fixed at 2 to 4 hours after reperfusion (**e, f**). **g.** 2,3-5-Triphenyl tetrazolium chloride staining of an ischemic rat brain 12 hours after reperfusion was shown to indicate the positions where the images (**a–f**) were obtained. The red asterisk in **g** indicated the places where the images (**a–d**) were obtained, which indicates the ischemic core in the striatum. The brain region surrounded by dashed line indicates the area where the typical translocation of HMGB1 was observed at a time point of 4 hours after reperfusion. **B.** HMGB1 translocated occurs in neurons but conserved in astrocytes and microglia cells even in the later phase of reperfusion. Sections were double stained with anti-HMGB1 antibody (Ab) and antimicrotubule-associated protein 2 (MAP2) Ab, antiglial fibrillary acidic protein (GFAP) Ab, or anti-ionized calcium-binding adaptor molecule 1 (Iba1) Ab. 4',6-Diamidino-2-phenylindole (blue) staining was used to show nuclear localization. All images were obtained from the cerebral cortex of the rat brain. Scale bars=50  $\mu$ m.

### In Vivo Brain Microdialysis

Rats were anesthetized using the same condition of the MCAO procedure and placed in a stereotaxic apparatus. Guide cannulae were implanted into the striatum (posterior, 0.25 mm; lateral, 4.0 mm from bregma; below the skull surface, 7.0 mm). Microdialysis probes (Eicom Co, Kyoto, Japan) were inserted through the guide cannulae. The probe was perfused with Ringer solution, and the microdialysis samples were collected. Glutamate in the samples was detected using a Shimadzu high-performance liquid chromatography system (Shimadzu Co, Kyoto, Japan) equipped with a C18 column (TSK-gel ODS-100V; Tosoh Bioscience, Tokyo, Japan).<sup>17</sup> Before experiments, the *in vitro* recovery of each microdialysis probe was determined and all probes had 14% recovery at a flow rate of 4  $\mu$ L/min. See detail in Supplemental Methods.

### Statistical Analysis

Statistical significance was evaluated using 2-way analysis of variance followed by the Student *t* test. The statistical significance of the microdialysis experiments for glutamate was evaluated using 1-factor repeated-measures analysis of variance. The statistical significance of *in vitro* BBB experiments was evaluated using analysis of variance followed by Dunnett test. A probability value of <0.05 was considered to be significant.

## Results

### HMGB1 Translocation and Release

Immunohistochemical staining of HMGB1 showed that HMGB1 was localized solely in the nuclear compartment with the spotted staining of nucleoli throughout the brain from sham-operated rats (Figure 1Aa). After the onset of ischemia, HMGB1 was time-dependently translocated and released from the nucleus (Figure 1Ab–d). One hour after the onset of ischemia, HMGB1 changed its distribution inside the nucleus, forming a “lotus root-like structure,” suggesting the rapid reorganization of HMGB1 within the nucleus (Figure 1Ab). Two hours after the onset of ischemia, cells in the ischemic core had shrunk, to some extent, and HMGB1 was stained both in cytoplasm and the nucleus suggesting the translocation of HMGB1 (Figure 1Ac). Two hours after reperfusion, HMGB1 staining was partially lost in the ischemic core area (Figure 1Ad). The typical translocation of HMGB1 into the cytosolic compartment was evident in the ischemic core at 2 hours after reperfusion (Figure 1Ae) and peaked at 4 hours after reperfusion (Figure 1Af). Double immunostaining of HMGB1 and

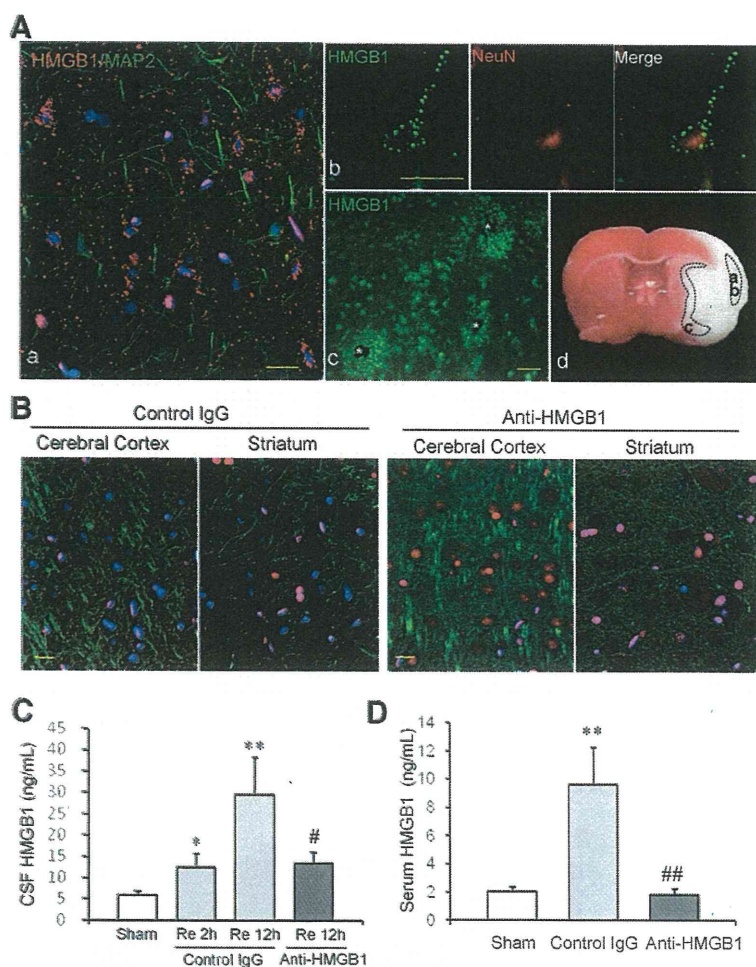


**Figure 2.** Translocation and release of high mobility group box-1 (HMGB1) from neurons and its inhibition by anti-HMGB1 monoclonal antibody (mAb). Coronal sections were prepared 12 hours after reperfusion. 4',6-Diamidino-2-phenylindole staining was performed to show the cell nuclei. **A**, HMGB1 was stained as a granule-like structure. **a**, HMGB1 (red) was stained as a granule-like structure aligning the neuron cell soma in the cerebral cortex. **b**, A representative cell stained both by anti-HMGB1 (green) and anti-NeuN Ab (red). **c**, HMGB1 staining (green) surrounding capillaries (asterisks) in the hypothalamus of the ischemia hemisphere. **d**, A 2-3-5-triphenyl tetrazolium chloride staining of an ischemic rat brain 12 hours after reperfusion was used to indicate the position where the corresponding images were obtained. The brain region surrounded by dashed line indicates the areas where the typical granule-like staining of HMGB1 were observed. Scale bars=20  $\mu$ m. **B**, Representative confocal images showing the inhibitory effects of the anti-HMGB1 mAb on HMGB1 translocation (red, HMGB1; green, microtubule-associated protein 2 [MAP2]). Scale bars=50  $\mu$ m. **C**, The HMGB1 levels in cerebrospinal fluid were determined using enzyme-linked immunosorbent assay (ELISA). The results are mean $\pm$ SEM of 10 (sham), 8 (2 hours in control IgG-treated group), and 9 (12 hours in control IgG-treated group), and 9 (anti-HMGB1 mAb-treated group) rats. **D**, Serum levels of HMGB1 at 12 hours after reperfusion were determined using ELISA. The results are mean $\pm$ SEM of 8 (sham), 8 (control IgG-treated group), and 9 (anti-HMGB1 mAb-treated group) rats. \*\* $P$ <0.01 compared with sham control. # $P$ <0.05 and ## $P$ <0.01 compared with the group treated with control IgG (reperfusion).

microtubule-associated protein 2 revealed that the translocation mostly occurred in neurons (Figure 1B). In contrast, HMGB1 immunoreactivities in astrocytes and microglial cells were retained in nuclei even in the late phase of reperfusion (Figure 1B). Interestingly, in the ischemic core of the cerebral cortex, we observed a granule-like staining pattern of HMGB1 aligned on the neuronal cell soma, especially in the late phase of reperfusion (Figure 2Aa–b). In addition, the considerable number of small granule-like HMGB1 staining was observed surrounding the capillaries, especially in the hypothalamus of the ischemic hemisphere (Figure 2Ac). Figure 2B shows that at 12 hours after reperfusion, HMGB1 staining was almost completely lost in most of the cells in the ipsilateral side of the brain when compared with the rats treated with control IgG. In contrast, treatment with the anti-HMGB1 mAb inhibited the translocation and disappearance of HMGB1. Consistent with the results of immunostaining, we found that the HMGB1 level in the ischemic core area of the rat brain 12 hours after reperfusion significantly decreased to 40% and 44% in the striatum and the cerebral cortex, respectively, compared with the sham-operated rat (Supplemental Figure I).

Determination of HMGB1 using enzyme-linked immunosorbent assay showed that HMGB1 appeared in the cerebrospinal fluid as early as 2 hours after reperfusion and increased to 30 ng/mL 12 hours after reperfusion. Treatment

with anti-HMGB1 mAb significantly decreased the HMGB1 levels in cerebrospinal fluid (Figure 2C). Western blot analysis also supported that HMGB1 time-dependently increased in the cerebrospinal fluid (Supplemental Figure II). The increase of serum HMGB1 levels after ischemia was also observed in rats treated with control IgG, but the serum levels of HMGB1 were suppressed in anti-HMGB1 mAb-treated rats to the same level as in sham-operated rats (Figure 2D). To clarify whether the therapeutic anti-HMGB1 mAb affected the HMGB1 enzyme-linked immunosorbent assay results, we coincubated the anti-HMGB1 mAb with HMGB1 in rat brain homogenate or rHMGB1 and examined the incubated samples in the enzyme-linked immunosorbent assay plate. The results clearly show that the therapeutic mAb had no effects on the enzyme-linked immunosorbent assay (Supplemental Figure III). Meanwhile, in the anti-HMGB1 mAb-treated MCAO rats, levels of plasma 4-HNE adducts were also significantly reduced by 61% compared with that in control IgG-treated MCAO rats (Supplemental Figure IV).

#### Alleviation of Brain Edema

Brain edema is defined as an abnormal accumulation of fluid within the brain parenchyma, producing a volumetric enlargement of brain cells or tissue, which is one of the primary causes of clinical deterioration and a leading cause of death

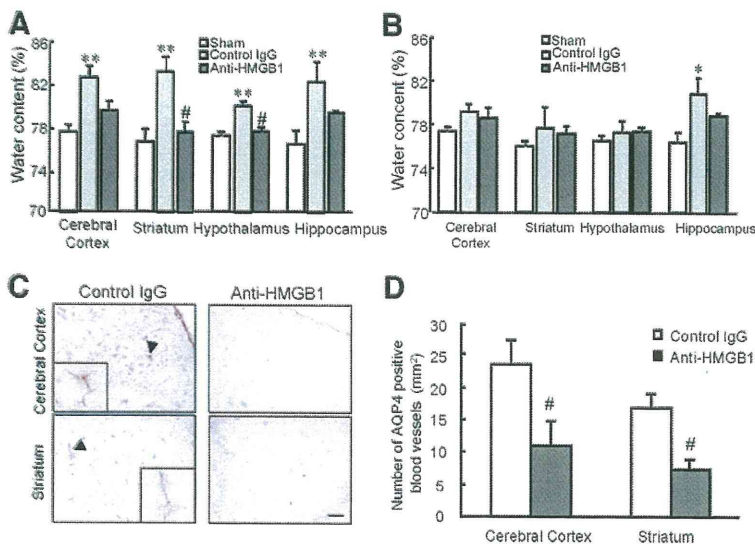


**Figure 3.** Brain water contents in rats treated with control IgG or anti-high mobility group box-1 (HMGB1) monoclonal antibody (mAb) at 3 hours after reperfusion. **A**, Ipsilateral hemisphere; **B** contralateral hemisphere. The results are mean±SEM of the data from 4 (sham), 8 (control IgG-treated group), and 9 (anti-HMGB1 mAb-treated group) rats. \**P*<0.05 and \*\**P*<0.01 compared with the sham-operated group. #*P*<0.05 compared with control IgG group. **C**, Immunohistochemical staining of aquaporin 4 (AQP4) in the brain sections from 2-hour middle cerebral artery occlusion (MCAO) rats. The rats were treated with the anti-HMGB1 or control mAb immediately after reperfusion. The tissues were fixed by infusing formalin transcardially at 3 hours after reperfusion. Coronal frozen sections were stained with an anti-AQP4 mAb as described in "Methods." Insets represent the higher magnification picture of indicated structure by arrows. Scale bar=100 μm. **D**, Quantitative results of AQP4 staining by counting the AQP4-positive blood vessels. The results are mean±SEM of the data from 5 rats. #*P*<0.05 compared with the control IgG group.

after ischemia/reperfusion. In the sham group, the brain water content formed 76% to 78% of the total weight. Three hours after reperfusion, in the rats treated with control IgG, the brain water contents in the cerebral cortex, striatum, hypothalamus, and hippocampus of the ischemic hemisphere had significantly increased to 82.8%, 83.3%, 80.0%, and 82.3%, respectively. In contrast, the anti-HMGB1 mAb attenuated the increase in water content by 3.2%, 5.7%, 2.3%, and 2.85% in each region, respectively (Figure 3A). The hippocampal edema occurred not only in the ischemic side, but also in the nonischemic side that was also inhibited by treatment with the anti-HMGB1 mAb (Figure 3B).

AQP4 is a prominent biological marker to determine the permeability of brain capillaries in brain edema.<sup>18,19</sup> Figure 3C shows that in the MCAO rats (3 hours after reperfusion) treated with control IgG, the immunoreactivity of AQP4 in the cerebral cortex and striatum was significantly increased. It appears that AQP4 was strongly expressed in capillary vessels, probably on the astroglial membranes<sup>20</sup> that had direct contact with the lamina propria. The results of AQP4 immunohistochemistry were quantitatively determined by counting the AQP4-positive blood vessels (Figure 3D). The treatment with anti-HMGB1 mAb remarkably inhibited the expression of AQP4 both in the cerebral cortex and striatum.

**MRI Studies**

MRI is considered the most promising and noninvasive tool for recognizing brain edema formation in real time. T2-weighted MRI is frequently used to determine the presence or absence of edema, especially vasogenic edema induced by reperfusion.<sup>21</sup> Consistent with the data for brain edema determined by the water content, T2-weighted MRI clearly showed time-dependent changes in brain edema in the ischemic areas containing the striatum, cerebral cortex, and hippocampus in the control rats. The representative data from 5 rats are shown in Figure 4A. Three hours after reperfusion, striatal edema was evident in the control Ab group. At 6 hours after reperfusion, the edematous areas had expanded to the cerebral cortex. Treatment with the anti-HMGB1 mAb inhibited the increase in the intensity of the images in the ischemic

areas (Figure 4A). Figure 4B summarizes the quantitative analysis of MRI based on intensity analysis of the images in the ischemic hemisphere against those in the contralateral hemisphere. At 24 hours after reperfusion, the high intense T2 signal in the control rats may contain a necrotic area. Before Ab treatment, the physiological parameters such as the neurological scores and Rotorod test scores were not different

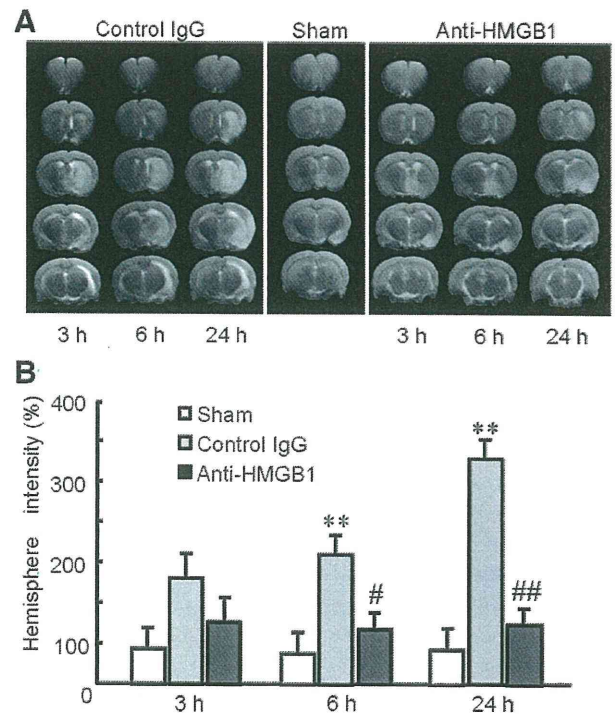


**Figure 4.** Serial T2-weighted MRI obtained from rats treated with control IgG or anti-high mobility group box-1 (HMGB1) monoclonal antibody (mAb). **A**, Representative MRI from rats in the control, anti-HMGB1, and sham groups. Time points indicate the intervals after reperfusion. **B**, Percentage of the intensity in the ipsilateral hemisphere against that in the contralateral hemisphere at various time points after reperfusion. The results are mean±SEM of 5 animals in each group. \**P*<0.05 and \*\**P*<0.01 compared with sham; #*P*<0.05 and ###*P*<0.01 compared with the control group.



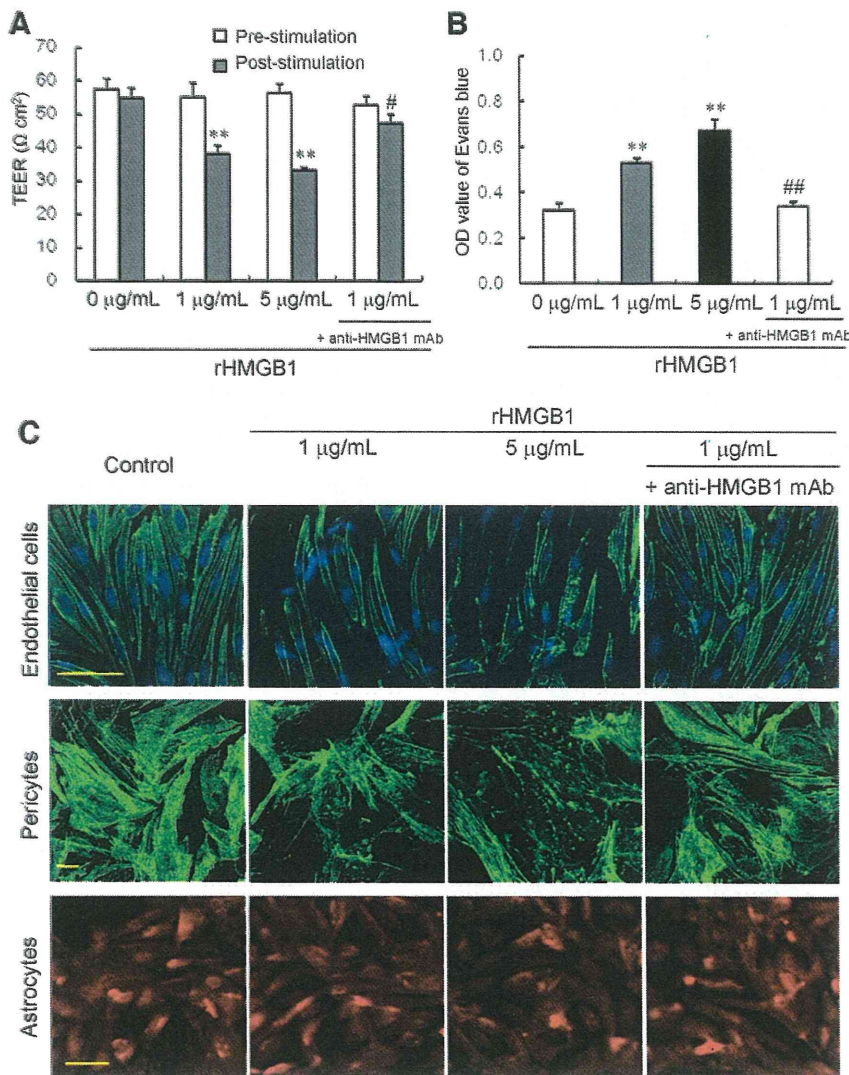


**Figure 5.** Effects of recombinant high mobility group box-1 (rHMGB1) on the permeability of rat reconstituted blood-brain barrier (BBB) in vitro. The rat-reconstituted BBB system composed of vascular endothelial cells, pericytes, and astrocytes was used for the experiments. **A**, Recombinant HMGB1 at 1 or 5 μg/mL was added to the brain side (lower chamber), and the incubation continued for 60 minutes. When the anti-HMGB1 monoclonal antibody (mAb) was added, the mAb at 2 μg/mL was preincubated with rHMGB1 for 30 minutes. Transendothelial electric resistance (TEER) was measured before and after HMGB1 stimulation. The results are mean ± SEM of 3 independent experiments. \*\**P* < 0.01 compared with the corresponding value before stimulation. #*P* < 0.05 compared with the value in the presence of rHMGB1 (1 μg/mL) alone. **B**, After the detection of TEER, Evans blue with albumin was added to the insert well and the incubation continued for 30 minutes. The transudated Evans blue dye into the lower chamber was determined. The results are mean ± SEM of 3 independent experiments. \*\**P* < 0.01 compared with the value in the absence of rHMGB1. ##*P* < 0.01 compared with the value in the presence of rHMGB1 (1 μg/mL) alone. **C**, After 1 hour stimulation with rHMGB1, the cells were fixed with 4% paraformaldehyde for 30 minutes. Endothelial cells and pericytes were labeled with alexa-488-phalloidin and 4',6-diamidino-2-phenylindole and observed under confocal microscope. Astrocytes were observed by Evans blue fluorescence. Scale bars = 50 μm.

between the anti-HMGB1 mAb and control IgG-treated groups (data not shown).

**In Vitro BBB Permeability Assay**

Using an in vitro BBB system composed of rat brain vascular endothelial cells, pericytes, and astrocytes, the direct effects of rHMGB1 on the permeability of BBB were examined (Figure 5). The rHMGB1 generated from inset cells (free of lipopolysaccharide) was added into the brain side (lower chamber) at a concentration of 1 μg/mL and 5 μg/mL, and the incubation continued for a total of 60 minutes. The addition of rHMGB1 concentration-dependently decreased the transendothelial electric resistance, and mAb antagonized the reduction of transendothelial electric resistance induced by rHMGB1, whereas the transendothelial electric resistance levels before stimulation were the same among groups (Figure 5A). The stimulation with rHMGB1 concentration-dependently increased the permeability of the Evans blue-albumin complex. The mAb significantly inhibited the enhanced permeability of BBB indicated by Evans blue-albumin leakage (Figure 5B).

Consistent with the results of the dye leakage and the reduction of transendothelial electric resistance, the stimulation

with rHMGB1 induced the morphological changes in pericytes and endothelial cells. In pericytes, the F-actin staining reduced after the stimulation with rHMGB1 concentration-dependently. Also, the vascular endothelials seemed to shrink longitudinally, leading to the intercellular space formation. These morphological effects of rHMGB1 were antagonized by the addition of anti-HMGB1 mAb. In contrast, there was no difference in astrocyte shape among groups examined (Figure 5C).

**Electron Microscopic Observation of the BBB**

Images from transmission electron microscopy clearly identified the BBB unit composed of endothelial cells, basal lamina, pericytes, and astrocyte end feet. Figure 6A shows representative images of the BBB unit in the striatum. In the control IgG rat brains fixed at 3 hours after reperfusion, it is evident that the astrocyte end feet were swollen to various extents in the ischemic regions (Figure 6Aa-b). In many cases, the intracellular organelles were absent or scarce in such swollen astrocyte end feet labeled by asterisks in Figure 6Aa. In addition to the enlargement of astrocyte end feet, the detachment of the end feet plasma membrane from the basal lamina was observed (arrows

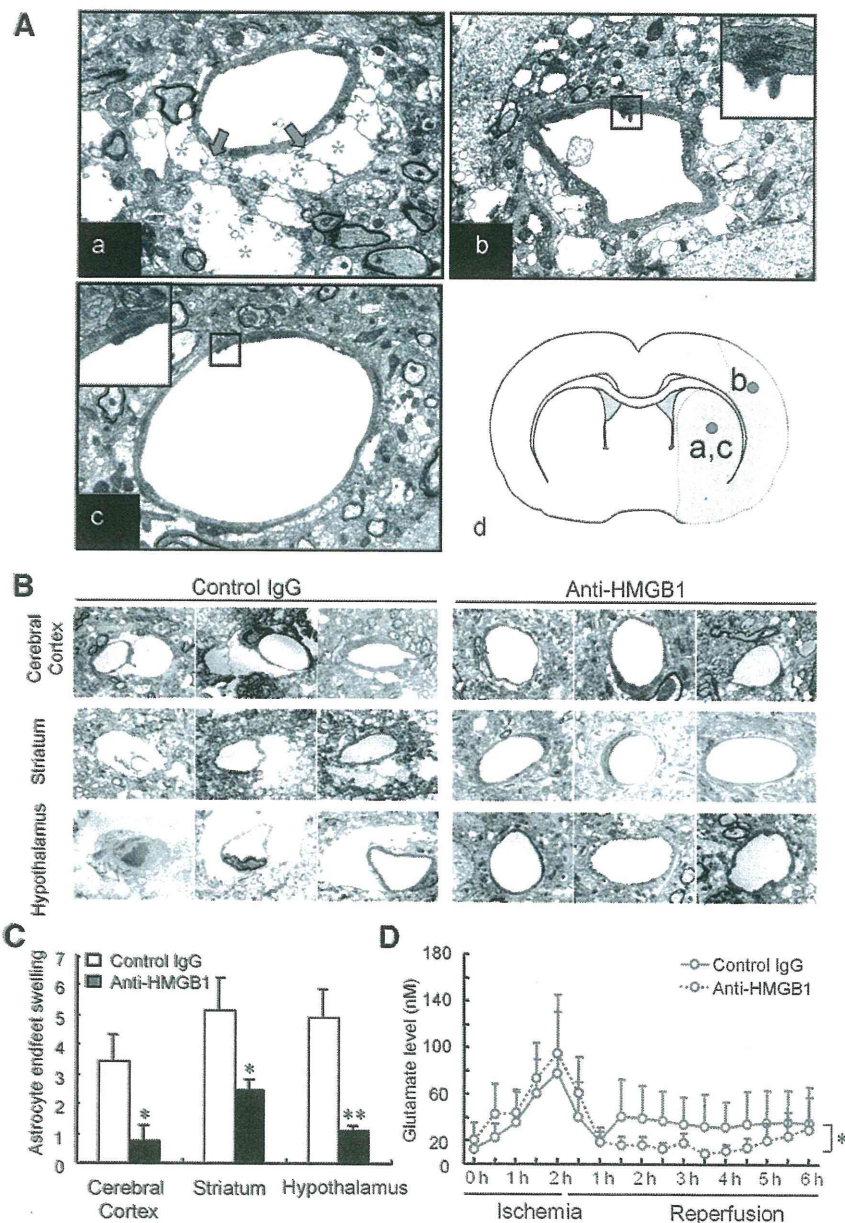


**Figure 6.** Ultrastructure of the blood-brain barrier (BBB) in the ischemic hemisphere obtained using transmission electron microscopy. **A.** Representative images of the coronal sections from rat brain treated with control IgG (**a, b**) or anti-high mobility group box-1 (HMGB1) monoclonal antibody (mAb; **c**) at 3 hours after reperfusion. **a.** Astrocyte end feet swelling and detachment. Asterisks indicate the swollen astroglial end feet. Arrows indicate the detachment of astrocyte end feet from the basal lamina. **b.** Tight junction deformation. The inserts shows a higher magnification of detached tight junction. **c.** A BBB unit in the anti-HMGB1 mAb-treated rat brain. The inserts show an intact tight junction. **d.** A scheme showing the places where the images (**a-c**) were obtained. **B.** Representative images for the quantitative analysis of the astrocyte end feet swelling in the rats treated with control IgG or anti-HMGB1 mAb. **C.** Quantitative results of astrocyte end feet swelling in each region were determined as described in the "Methods." The results are mean ± SEM of 7 capillaries in each area of 8 rats from each group. \* $P < 0.05$  and \*\* $P < 0.01$  compared with the control group (original magnification ×8000). **D.** Extracellular levels of glutamate in microdialysis samples during and after brain ischemia. The rats were treated with control IgG or anti-HMGB1 mAb immediately after reperfusion. Each point represents mean ± SEM of 4 rats. The statistical analysis was performed by comparing the time course changes of each group at 1 hour after reperfusion up to 6 hours using 1-factor repeated-measures analysis of variance. \* $P < 0.05$  compared with the control group.

in Figure 6Aa). Electron-dense TJ structures between the capillary endothelial cells were deformed and the gap clefts were seen in the control IgG-treated rats (Figure 6Ab). Treatment with the anti-HMGB1 mAb remarkably protected the BBB structures from the enlargement of the astrocyte end feet, detachment of the end feet plasma membrane from the basal lamina, and the deformation of the TJ (Figure 6Ac). To quantitatively evaluate the effect of the anti-HMGB1 mAb on astrocyte swelling in the different brain regions, we measured the ratio of the area of the swollen astrocyte end feet against a capillary luminal area. Figure 6B shows 3 representative images of the calculated astrocyte end feet from the relative brain regions. The results indicate that astrocyte end feet swelling was significantly inhibited by treatment with the anti-HMGB1 mAb (Figure 6C).

High levels of extracellular glutamate can lead to disruption of the BBB and consequently to vasogenic edema.<sup>22,23</sup>

Thus, we detected the extracellular levels of glutamate in the striatum using a microdialysis-high-performance liquid chromatography technique. We found that extracellular glutamate decreased immediately after blood reflow induced by reperfusion. However, at 1 hour after reperfusion, a secondary increase of glutamate was detected persisted for up to 6 hours after reperfusion, which may be induced by the secondary injury induced by reperfusion.<sup>24,25</sup> Impressively, treatment with the anti-HMGB1 mAb significantly inhibited the sustained elevation of extracellular glutamate (Figure 6D).

### Discussion

In the present study, we provided further evidence for the therapeutic effects of anti-HMGB1 mAb on brain edema and BBB disruption induced by brain ischemic insult. Electron microscopic observation in the 2-hour MCAO rat model

demonstrated the swelling of astrocyte end feet, the detachment of the plasma membrane astrocyte end feet from the basal lamina, and the loosening of the TJ between capillary endothelial cells occurred at 3 hours after reperfusion. T2-weighted MRI at 3 hours after reperfusion was consistent with the electron microscope findings. This may indicate that the therapeutic approach to an ischemic brain injury should contain an aspect to control this rapid and drastic disruption of the BBB. In fact, anti-HMGB1 mAb therapy efficiently ameliorated these changes to the BBB structure. Thus, the decrease in protein leakage identified in our previous study was due to the effects of the anti-HMGB1 mAb on BBB maintenance.<sup>9</sup>

Using an *in vitro* BBB system, we clearly demonstrated that rHMGB1 increased the vascular permeability of the BBB to the Evans blue–albumin complex associated with the morphological changes in endothelial cells and pericytes. Thus, the significant inhibitory effects of anti-HMGB1 mAb on rHMGB1 action *in vitro* probably reflect the *in vivo* condition after ischemic insult. HMGB1 once released into the extracellular space surrounding capillary vessels therefore may induce BBB disruption directly by acting on its component cells. Further work is necessary to determine whether HMGB1 affects both endothelial cells and pericytes at the same time or in order.

In the present study, we clearly showed that HMGB1 translocation was time-dependent and cell type-specific. In the case of neurons, the time-dependent translocation of HMGB1 can be summarized into 3 steps: (1) its redistribution inside the nucleus; (2) the translocation of HMGB1 from the nucleus into the cytosolic compartment; and (3) the release of HMGB1 into the extracellular space. The typical translocation of HMGB1 from the nucleus to the cytoplasm was observed at 2 to 4 hours after reperfusion, which is consistent with the findings obtained by other groups using the mouse MCAO model.<sup>10,11</sup> Thus, the intranuclear and cytosolic translocation and then extracellular release of HMGB1 probably take place in the majority of neurons under ischemic conditions. The translocation of HMGB1 may be the result of the chemical modification of HMGB1 such as acetylation, phosphorylation, or methylation.<sup>26–28</sup> There may be such modifications under ischemic conditions, although the signaling cascades required to trigger the activation of the necessary enzymes remain to be determined.

Another interesting finding in this study is that we observed a special granule-like structure of HMGB1 aligned on the neuronal cell soma in the ischemic core area in the cerebral cortex. It appears that HMGB1 may be taken up into vesicular structures in the cytoplasm. These vesicular structures may bind to the plasma membrane judging from their distribution pattern depicting cell soma. At this time, we do not know the nature of the vesicular structures, that is, endosome, lysosome, mitochondria, or fused synaptic vesicles. Further study is needed to identify the vesicles using double immune staining of HMGB1 and specific markers of vesicles to clarify this point. In the present study, we used a transient occlusion model; however, permanent MCAO may show a different pattern of HMGB1 translocation and BBB disruption. Therefore, the effects of anti-HMGB1 mAb on a permanent MCAO model should be examined experimentally.

Using a microdialysis–high-performance liquid chromatography technique, we detected a rapid elevation of glutamate during ischemia. The second elevation of glutamate was detected at 1 hour after reperfusion. Interestingly, treatment with the anti-HMGB1 mAb significantly inhibited the second increase in glutamate. It was also reported that glutamate can induce the release of HMGB1 from neuronal cells *in vitro*.<sup>10</sup> The released HMGB1 probably facilitated the disruption of BBB as demonstrated in the present study, leading to brain edema. The resultant increase in brain tissue pressure as well as gas-diffusion barrier formation will exacerbate the neuronal damage, leading to glutamate release. Therefore, neutralization of HMGB1 by mAb will reduce the BBB damage, glutamate release, and HMGB1 translocation at the same time.

The rapid increase in HMGB1 levels in the cerebrospinal fluid as well as the HMGB1 translocation demonstrated by immunohistochemistry supported that a considerable amount of HMGB1 was released into the extracellular space. Moreover, we observed a marked increase in the serum levels of HMGB1 after the ischemic brain insult. This finding was consistent with the data reported by others.<sup>8,29</sup> We also determined the effect of the anti-HMGB1 mAb on serum HMGB1 levels and found that the therapy dramatically reduced serum HMGB1 levels to those observed in sham rats. To examine the possibility that the therapeutically administered anti-HMGB1 mAb interfered with the sandwich enzyme-linked immunosorbent assay, we added the therapeutic mAb to this assay together with the standard HMGB1 preparation. The anti-HMGB1 mAb as well as an anti-KLH mAb had no influence on enzyme-linked immunosorbent assay (Supplemental Figure III). Therefore, we concluded that the intravenously injected anti-HMGB1 mAb binds to circulating HMGB1 and facilitates its clearance from the bloodstream.

HMGB1 released in circulation may increase the inflammatory response to the endothelial cells of the vulnerable BBB.<sup>30</sup> It is well established that oxidative stress during focal cerebral ischemia is one of the major contributors to the disruption of BBB and secondary brain damage.<sup>31–33</sup> The serum HMGB1 released from the ischemic brain may stimulate the production of proinflammatory cytokines in monocytes or activate vascular endothelial cells, which may produce high amounts of reactive oxygen species.<sup>30,34</sup> The reactive oxygen species in turn induces protein and lipid oxidation (Supplemental Figure IV) in the blood. The elimination of HMGB1 from circulation by the anti-HMGB1 mAb must be another important mechanism for the effects of mAb therapy. At this time, we do not know the relative contribution of this effect of the anti-HMGB1 mAb to the total beneficial effects of the Ab; however, it is possible that clearance of the HMGB1 antigen may inhibit the procoagulant effect of HMGB1, the activation of vascular endothelial cells, and monocyte activation.<sup>9,34,35,36</sup>

In conclusion, mAb treatment against HMGB1 may provide a new strategy for brain infarction by inhibiting important inflammatory responses in addition to thrombolytic tissue plasminogen activator.

### Acknowledgments

We thank Dr Kazushi Kinugasa for his discussion on the article and Mr Hiroshi Okamoto and Mr Masahiro Narasaki for their technical assistance.

### Sources of Funding

This work was supported by grants from the Scientific Research from the Ministry of Health, Labor and Welfare of Japan, from the Japan Society for the Promotion of Science (JSPS No. 21390071, 21590594, 21659141), and from the Okayama Prefecture Foundation for Promotion of Industry.

### Disclosures

None.

### References

- Zhang ZG, Zhang L, Jiang Q, Zhang R, Davies K, Powers C, Bruggen N, Chopp M. VEGF enhances angiogenesis and promotes blood-brain barrier leakage in the ischemic brain. *J Clin Invest*. 2000;106:829–838.
- Han F, Shirasaki Y, Fukunaga K. Microsphere embolism-induced endothelial nitric oxide synthase expression mediates disruption of the blood-brain barrier in rat brain. *J Neurochem*. 2006;99:97–106.
- Liu T, Clark RK, McDonnell PC, Young PR, White RF, Barone FC, Feuerstein GZ. Tumor necrosis factor- $\alpha$  expression in ischemic neurons. *Stroke*. 1994;25:1481–1488.
- Saito K, Suyama K, Nishida K, Sei Y, Basile AS. Early increases in TNF- $\alpha$ , IL-6 and IL-1 beta levels following transient cerebral ischemia in gerbil brain. *Neurosci Lett*. 1996;206:149–152.
- Wang H, Bloom O, Zhang M, Vishnubhakat JM, Ombrellino M, Che J, Frazier A, Yang H, Ivanova S, Borovikova L, Manogue KR, Faist E, Abraham E, Andersson J, Andersson U, Molina PE, Abumrad NN, Sama A, Tracey KJ. HMG-1 as a late mediator of endotoxin lethality in mice. *Science*. 1999;285:248–251.
- Abraham E, Arcaroli J, Carmody A, Wang H, Tracey KJ. HMG-1 as a mediator of acute lung inflammation. *J Immunol*. 2000;165:2950–2954.
- Taniguchi N, Kawahara K, Yone K, Hashiguchi T, Yamakuchi M, Goto M, Inoue K, Yamada S, Ijiri K, Matsunaga S, Nakajima T, Komiya S, Maruyama I. High mobility group box chromosomal protein 1 plays a role in the pathogenesis of rheumatoid arthritis as a novel cytokine. *Arthritis Rheum*. 2003;48:971–981.
- Kim JB, Sig Choi J, Yu YM, Nam K, Piao CS, Kim SW, Lee MH, Han PL, Park JS, Lee JK. HMGB1, a novel cytokine-like mediator linking acute neuronal death and delayed neuroinflammation in the posts ischemic brain. *J Neurosci*. 2006;26:6413–6421.
- Liu K, Mori S, Takahashi HK, Tomono Y, Wake H, Kanke T, Sato Y, Hiraga N, Adachi N, Yoshino T, Nishibori M. Anti-high mobility group box 1 monoclonal antibody ameliorates brain infarction induced by transient ischemia in rats. *FASEB J*. 2007;21:3904–3916.
- Qiu J, Nishimura M, Wang Y, Sims JR, Qiu S, Savitz SI, Salomone S, Moskowitz MA. Early release of HMGB-1 from neurons after the onset of brain ischemia. *J Cereb Blood Flow Metab*. 2008;28:927–938.
- Kim JB, Lim CM, Yu YM, Lee JK. Induction and subcellular localization of high-mobility group box-1 (HMGB1) in the posts ischemic rat brain. *J Neurosci Res*. 2008;86:1125–1131.
- Muhammad S, Barakat W, Stoyanov S, Murikinati S, Yang H, Tracey KJ, Bendszus M, Rossetti G, Nawroth PP, Bierhaus A, Schwanninger M. The HMGB1 receptor RAGE mediates ischemic brain damage. *J Neurosci*. 2008;28:12023–12031.
- Yang Y, Estrada EY, Thompson JF, Liu W, Rosenberg GA. Matrix metalloproteinase mediated disruption of tight junction proteins in cerebral vessels is reversed by synthetic matrix metalloproteinase inhibitor in focal ischemia in rat. *J Cereb Blood Flow Metab*. 2007;27:697–709.
- Piao MS, Lee JK, Park CS, Ryu HS, Kim SH, Kim HS. Early activation of matrix metalloproteinase-9 is associated with blood-brain barrier disruption after photothrombotic cerebral ischemia in rats. *Acta Neurochir (Wien)*. 2009;151:1649–1653.
- Lai YL, Smith PM, Lamm WJ, Hildebrandt J. Sampling and analysis of cerebrospinal fluid for chronic studies in awake rats. *J Appl Physiol*. 1983;54:1754–1757.
- Nakagawa S, Deli MA, Kawaguchi H, Shimizudani T, Shimono T, Kittel A, Tanaka K, Niwa M. A new blood-brain barrier model using primary rat brain endothelial cells pericytes and astrocytes. *Neurochem Int*. 2009;54:253–263.
- Ishide T, Mancini M, Maher TJ, Chayaikul P, Ally A. Rostral ventrolateral medulla opioid receptor activation modulates glutamate release and attenuates the exercise pressor reflex. *Brain Res*. 2000;865:177–185.
- Jung JS, Bhat RV, Preston GM, Guggino WB, Baraban JM, Agre P. Molecular characterization of an aquaporin cDNA from brain: candidate osmoreceptor and regulator of water balance. *Proc Natl Acad Sci U S A*. 1994;91:13052–13056.
- Papadopoulos MC, Verkman AS. Aquaporin-4 and brain edema. *Pediatr Nephrol*. 2007;22:778–784.
- Nielsen S, Nagelhus EA, Amiry-Moghaddam M, Bourque C, Agre P, Ottersen OP. Specialized membrane domains for water transport in glial cells: high-resolution immunogold cytochemistry of aquaporin-4 in rat brain. *J Neurosci*. 1997;17:171–180.
- Juránek I, Baciak L. Cerebral hypoxia-ischemia: focus on the use of magnetic resonance imaging and spectroscopy in research on animals. *Neurochem Int*. 2009;54:471–480.
- Mayhan WG, Didion SP. Glutamate-induced disruption of the blood-brain barrier in rats. Role of nitric oxide. *Stroke*. 1996;27:965–969.
- Preston E, Webster J. A two-hour window for hypothermic modulation of early events that impact delayed opening of the rat blood-brain barrier after ischemia. *Acta Neuropathol*. 2004;108:406–412.
- Jean WC, Spellman SR, Nussbaum ES, Low WC. Reperfusion injury after focal cerebral ischemia: the role of inflammation and the therapeutic horizon. *Neurosurgery*. 1998;43:1382–1396.
- Siesjö BK, Siesjö P. Mechanisms of secondary brain injury. *Eur J Anaesthesiol*. 1996;13:247–268.
- Bonaldi T, Talamo F, Scalfidi P, Ferrera D, Porto A, Bachi A, Rubartelli A, Agresti A, Bianchi ME. Monocytic cells hyperacetylate chromatin protein HMGB1 to redirect it towards secretion. *EMBO J*. 2003;22:5551–5560.
- Youn JH, Shin JS. Nucleocytoplasmic shuttling of HMGB1 is regulated by phosphorylation that redirects it toward secretion. *J Immunol*. 2006;177:7889–7897.
- Zhang Q, Wang Y. HMG modifications and nuclear function. *Biochim Biophys Acta*. 2010;1799:28–36.
- Hayakawa K, Mishima K, Irie K, Hazekawa M, Mishima S, Fujioka M, Orito K, Egashira N, Katsurabayashi S, Takasaki K, Iwasaki K, Fujiwara M. Camabidiol prevents a post-ischemic injury progressively induced by cerebral ischemia via a high-mobility group box1-inhibiting mechanism. *Neuropharmacology*. 2008;55:1280–1286.
- Fisher M. Injuries to the vascular endothelium: vascular wall and endothelial dysfunction. *Rev Neurol Dis*. 2008;5:S4–S11.
- Chan PH. Oxygen radicals in focal cerebral ischemia. *Brain Pathol*. 1994;4:59–65.
- Kondo T, Reaume AG, Huang TT, Carlson E, Murakami K, Chen SF, Hoffman EK, Scott RW, Epstein CJ, Chan PH. Reduction of CuZn-superoxide dismutase activity exacerbates neuronal cell injury and edema formation after transient focal cerebral ischemia. *J Neurosci*. 1997;17:4180–4189.
- Heo JH, Han SW, Lee SK. Free radicals as triggers of brain edema formation after stroke. *Free Radic Biol Med*. 2005;39:51–70.
- Andersson U, Wang H, Palmblad K, Aveberger AC, Bloom O, Erlandsson-Harris H, Janson A, Kokkola R, Zhang M, Yang H, Tracey KJ, Andersson U, Wang H, Palmblad K, et al. High mobility group 1 protein (HMG-1) stimulates proinflammatory cytokine synthesis in human monocytes. *J Exp Med*. 2000;192:565–570.
- Ito T, Kawahara K, Nakamura T, Yamada S, Nakamura T, Abeyama K, Hashiguchi T, Maruyama I. High-mobility group box 1 protein promotes development of microvascular thrombosis in rats. *J Thromb Haemost*. 2007;7:109–116.
- Treutiger CJ, Mullins GE, Johansson AS, Rouhiainen A, Rauvala HM, Erlandsson-Harris H, Andersson U, Yang H, Tracey KJ, Andersson J, Palmblad JE. High mobility group 1 B-box mediates activation of human endothelium. *J Intern Med*. 2003;254:375–385.

## 1 Supplemental Materials

### 2 Supplemental Methods

#### 3 Recombinant human HMGB1 (rHMGB1)

4 rHMGB1 was produced in Sf9 cells to obtain LPS-free HMGB1. In brief, full-length human  
5 HMGB1 DNA was amplified by PCR using Cap Site cDNA dT from human microvascular  
6 endothelial cells (Nippon Gene, Tokyo, Japan) and primers (forward 5'-GCA GAA TTC ATG  
7 GGC AAA GGA GAT CCT A-3', reverse 5'-CAT CTC GAG TCA TTA TTC ATC ATC ATC  
8 ATC-3'). The fragment was digested with EcoRI and XhoI and cloned into the  
9 pFastBacHTA (Invitrogen, Carlsbad, CA, USA) expression vector. The transfection of the Sf9  
10 cells with the pFastBacHTA-HMGB1 bacmid was performed according to the manufacturer's  
11 instructions (Bac-to-Bac Baculovirus Expression System, Invitrogen). The infected SF9 cell  
12 extract containing His-tagged HMGB1 protein was applied to Ni-NTA agarose (Qiagen,  
13 Hilden, Germany) and incubated for 3 hours at room temperature. After extensive washing,  
14 rHMGB1 was eluted with imidazole buffer. The rHMGB1 was collected and dialyzed  
15 overnight at 4 °C against PBS. Purified rHMGB1 protein was identified by SDS-PAGE and  
16 Western blotting with anti-HMGB1 mAb. (#10-22). The final HMGB1 preparation contained  
17 LPS of less than 2.0 pg/μg protein.

#### 18 Immunohistochemistry staining

19 Rats were anesthetized deeply with an i.p. injection of sodium pentobarbital (50mg/kg) and  
20 transcardially perfused by cold saline and then 10% formalin. Brains were post-fixed  
21 overnight in 10% formalin and paraffin-embedded. Brain sections were cut at a thickness of  
22 6 μm. An antigen retrieval procedure was performed in a 0.1 M sodium citric acid buffer  
23 (pH 6.0) by heating in autoclave at 120 °C for 10 min. After washing with tris-buffered  
24 saline (TBS), the sections were immersed in 10% normal goat serum (Sigma-Aldrich Co., St.  
25 Louis, MO, USA) in TBS containing 1% bovine serum albumin (BSA) for 2 h to block  
26 nonspecific binding. HMGB1 was stained using a mouse anti-HMGB1 mAb (R&D systems,  
27 Inc., Minneapolis, MN, USA) or a rabbit anti-HMGB1 Ab (Abcam plc, Cambridge, UK).  
28 For double immuno staining, the sections were incubated overnight with anti-HMGB1 mAb  
29 (R&D systems, Inc., Minneapolis, MN, USA) in combination with anti-microtubule  
30 associated protein 2 (MAP2) Ab (Santa Cruz Biotechnology, Inc., Santa Cruz, CA, USA),  
31 anti-gial fibrillary acidic protein (GFAP) Ab (Abcam plc, Cambridge, UK), or anti-ionized  
32 calcium-binding adaptor molecule 1 (Iba1) Ab (Wako, Inc, Osaka, Japan) as the primary  
33 antibodies at 4 °C. Alexa-555 labeled anti-mouse IgG (Invitrogen Co., Branford, CT, USA)  
34 and alexa-488 labeled anti-rabbit IgG (Invitrogen Co., Branford, CT, USA) were used as the  
35 secondary Abs. Sections were incubated with the secondary Ab at room temperature for 1 h  
36 and mounted using VECTORSHIELD Hard Set Mounting Medium with DAPI (Vector  
37 Laboratories, Inc., Burlingame, CA, USA). Stained sections were observed under an LSM  
38 510 confocal imaging system (Carl Zeiss, Inc., Jena, Germany). For aquaporin 4 (AQP4)  
39 staining, frozen sections of rat brains were prepared. A mouse anti-aquaporin 4 mAb (Abcam

1 plc, Cambridge, UK) was used as the primary Ab, followed by incubation with  
2 HRP-conjugated goat anti-mouse IgG (MBL international, Inc., Woburn, MA, USA).  
3 Diaminobenzidine (Sigma-Aldrich Co., St. Louis, MO, USA) and H<sub>2</sub>O<sub>2</sub> were used as the  
4 substrates for the reaction.

#### 5 **Western blotting for HMGB1 in cerebrospinal fluid**

6 Cerebrospinal fluid samples were collected from the cistern magna according to the  
7 previously reported method<sup>1</sup>. The samples were mixed with SDS-PAGE sample loading  
8 buffer under reducing condition. We loaded 15 µL of the samples per lane on SDS-PAGE.  
9 After transferring the proteins to a nitrocellulose membrane (Bio-Rad Laboratories, Inc.,  
10 Hercules, CA, USA), the membranes were blocked with TBS containing 0.1% Tween 20  
11 (T-TBS) and 10% skimmed milk, and then probed with the anti-HMGB1 mAb (#10-22)  
12 labeled by horseradish peroxidase using a Peroxidase Labeling Kit-NH2 (Dojindo Molecular  
13 Technologies, Inc., Kumamoto, Japan). After washing in T-TBS, an ECL system (Thermo  
14 Fisher Scientific Inc., Rockford, IL, USA) was used to visualize the HMGB1 band.

#### 15 **Western blotting using brain homogenate samples**

16 Rat brain samples were collected at the time point of 12 h after reperfusion. Brain slices  
17 were cut from 0.5 mm anterior from the bregma with the thickness of 2 mm. The ischemic  
18 core area in the striatum and the cortex indicated as Supplemental Figure 1B were cut and  
19 homogenized in cold Radio Immuno Precipitation Assay buffer (RIPA) (150 mM NaCl, 0.1%  
20 Triton X-100, 0.5% sodium deoxycholate, 0.1 % SDS, and 50 mM Tris-HCl, pH 8.0) with  
21 cocktail protease inhibitors (Sigma-Aldrich Co., St. Louis, MO, USA). The brain  
22 homogenate were then centrifuged at 10,000 g for 20 min. The protein concentration in the  
23 supernatant were detected by Bio-Rad Protein Assay (Bio-Rad Laboratories, Inc., Hercules,  
24 CA, USA), and adjusted to 250 µg/mL as the final concentration by Western sample buffer,  
25 10 µL of each sample was loaded to the SDS-PAGE. After transferring the proteins to a  
26 nitrocellulose membrane (Bio-Rad Laboratories, Inc., Hercules, CA, USA), the membranes  
27 were blocked with T-TBS and 10% skimmed milk, and then probed with the anti-HMGB1  
28 mAb (#10-22) labeled by horseradish peroxidase using a Peroxidase Labeling Kit-NH2  
29 (Dojindo Molecular Technologies, Inc., Kumamoto, Japan). β-actin was probed with a  
30 mouse anti-β-actin mAb (Santa Cruz Biotechnology, Inc., Santa Cruz, CA, USA ) followed  
31 by a HRP conjugated goat anti-mouse Ab. After washing in T-TBS, an ECL system  
32 (Thermo Fisher Scientific Inc., Rockford, IL, USA) was used to visualize the bands of  
33 HMGB1 and β-actin.

#### 34 ***In vitro* BBB permeability assay**

35 An *in vitro* BBB kit<sup>TM</sup> (RBE-12, PharmaCo-Cell Co. Ltd., Sakamoto, Japan) was used to  
36 assess the effects of rHMGB1 and the mAb to the BBB unit according to the instruction of  
37 the manufacturer<sup>2</sup>. The BBB system was composed of rat brain vascular endothelial cells,  
38 pericytes and astrocytes. The endothelial cells were cultured on the bottom of polyester

1 membrane (radius, 6 mm; thickness, 10  $\mu\text{m}$ ; pore size, 0.4  $\mu\text{m}$ ) of the insert well. The  
2 pericytes were present below the membrane of the insert well. The astrocytes were cultured  
3 on the bottom of the lower chamber. rHMGB1 expressed and purified from Sf9 insect cells.  
4 rHMGB1 alone or together with the anti-HMGB1 mAb after pre-incubation for 30 min was  
5 added into the lower chamber which is supposed to be the brain side. Trans Endothelial  
6 Electrical Resistance (TEER) was measured before and 30 min after stimulation with  
7 rHMGB1 using an EVOM resistance meter (World Precision Instruments, Sarasota, FL) as  
8 previously reported (Hiu *et al.*, 2008). The values are shown as  $\Omega \times \text{cm}^2$ . Thereafter,  
9 Evans' blue (165  $\mu\text{g}/\text{mL}$ ) bound to 0.1% BSA<sup>3</sup> was added to the insert well which is  
10 supposed to be the blood vessel side. The plate was further incubated for 30 min at 37°C.  
11 The media in the lower compartment was then collected, and the absorbance of Evans blue at  
12 595 nm was detected using a spectrophotometer (U-1500, Hitachi Ltd., Tokyo, Japan) to  
13 study the leakage of Evans blue-albumin complex.

14 The insert wells were washed by PBS, and the cells in the insert wells were fixed by 4%  
15 paraformaldehyde for 30 min at room temperature. The fixed cells were then washed by PBS  
16 and incubated with 0.1% Triton-X100 for 5 min at room temperature. An alexa-488 labeled  
17 phalloidin (Invitrogen Co., Branford, CT, USA) was added to the insert wells for F-actin  
18 staining. Cell nuclei were visualized by staining with DAPI (0.3  $\mu\text{M}$ ). The endothelial  
19 cells and pericytes in the insert wells were examined using a LSM 510 confocal imaging  
20 system (Carl Zeiss, Inc., Jena, Germany). The autofluorescence of Evans blue uptaken by  
21 astrocytes was observed in a fluorescence microscope (BZ-8000, Keyence Co., Osaka,  
22 Japan).

### 23 ***In vivo* brain microdialysis of glutamate**

24 Rats were anesthetized using the same condition of MCAO procedure. Rats were placed in  
25 a stereotaxic apparatus. Guide cannulae were implanted into the striatum (posterior: 0.25  
26 mm, lateral: 4.0 mm from bregma; below the skull surface: 7.0 mm) through a hole drilled in  
27 the skull and fixed with two anchor screws and dental cement. One week after surgery,  
28 microdialysis probes (Eicom Co., Kyoto, Japan) with a membrane length of 3 mm were  
29 carefully inserted through the guide cannulae. The probe was perfused at a flow rate of 4  
30  $\mu\text{L}/\text{min}$  with Ringer's solution ( $\text{Na}^+$ : 147 mM,  $\text{K}^+$ : 4 mM,  $\text{Ca}^{2+}$ : 4.5 mM,  $\text{Cl}^-$ : 155.5 mM).  
31 After a stabilization period (approximately 2–3 hours), the microdialysis samples were  
32 collected every 15 min before, during and after MCAO. Samples were precisely reacted  
33 with OPA working solution (OPA,  $\beta$ -ME, sodium tetraborate) for 4 min at 32°C according to  
34 the previously reported method<sup>4</sup>, and detected using a Shimadzu HPLC system (Shimadzu  
35 Co., Kyoto, Japan) equipped with a C18 column (TSKgel ODS-100V, Tosoh Bioscience,  
36 Tokyo, Japan) and a fluorescence detector (RF-530, Shimadzu Co., Japan). The mobile  
37 phase was 0.1 M  $\text{Na}_2\text{HPO}_4$  containing 25% methanol (pH 6.75 adjusted by  $\text{H}_3\text{PO}_4$ ). Before  
38 experiments, the *in vitro* recovery of each microdialysis probe was determined and all probes  
39 had 14% recovery at a flow rate of 4  $\mu\text{L}/\text{min}$ .

### 40 **Determination of 4-hydroxynonenal (4-HNE) adducts**

1 Plasma samples were prepared from 1 mL of blood collected via the inferior vena cava of  
2 sham and MCAO operated rats treated with control Ab or anti-HMGB1 mAb. The levels of  
3 4-HNE adducts in each sample were determined using an OxiSelect™ HNE-His Adduct  
4 ELISA Kit (Cell Biolabs, Inc., San Diego, CA, USA) with HNE-BSA as the standard. The  
5 determination was performed on triplicate samples.

6



1 **Supplemental Table**

2 Table 1. Basic physiological parameters for study groups.

	Pre	Control IgG		Anti-HMGB1	
		10 min	8 h	10 min	8 h
pH	7.4 ± 0.08	7.4 ± 0.01	7.4 ± 0.02	7.4 ± 0.01	7.3 ± 0.03
PCO <sub>2</sub> (mmHg)	43 ± 2.45	43.2 ± 1.35	46.4 ± 2.67	39.9 ± 1.99	42.9 ± 2.48
PO <sub>2</sub> (mmHg)	162.6 ± 17.6	170.6 ± 6.05	153.4 ± 6.17	148.5 ± 3.7#	156.1 ± 2.8
Base excess (mmol/L)	-0.5 ± 1.6	-1.1 ± 0.8	-0.7 ± 0.8	-0.7 ± 0.2	-2.5 ± 1.1
HCO <sub>3</sub> <sup>-</sup> (mmol/L)	22.4 ± 1.7	23.9 ± 0.7	24.7 ± 0.7	27.2 ± 3.8	22.7 ± 0.8
Hemoglobin (g/dl)	11.2 ± 0.6	12 ± 0.3	12.3 ± 0.9	11.1 ± 0.4	12.8 ± 0.3
Na <sup>+</sup> (mmol/L)	127 ± 2.4	130.8 ± 1.3	135.6 ± 0.7	130 ± 1.1	136 ± 1.6
K <sup>+</sup> (mmol/L)	3.8 ± 0.1	6.5 ± 0.7*	4.0 ± 0.1	3.4 ± 0.1#	3.6 ± 0.1
Ca <sup>2+</sup> (mmol/L)	0.8 ± 0.07	1.0 ± 0.06	1.1 ± 0.02	0.8 ± 0.07	1.1 ± 0.05
Cl <sup>-</sup> (mmol/L)	95 ± 1.2	102.8 ± 0.5	107.4 ± 0.8	99 ± 1.9	110 ± 2.4
Glucose (mg/dl)	158.6 ± 8.7	202.6 ± 13.9*	165.2 ± 9.7	176.8 ± 10.4	176.2 ± 7.4
Lactate (mg/L)	19.4 ± 1.5	18.2 ± 0.5	16 ± 1.2	16 ± 2.2	12.2 ± 1.1#

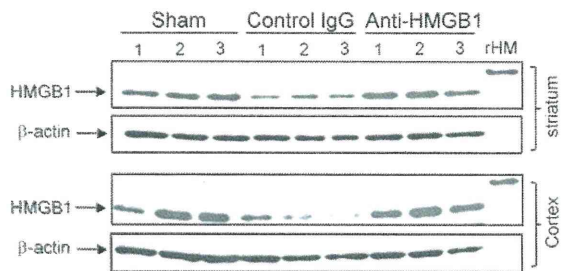
3 Control IgG or anti-HMGB1 mAb was administered intravenous under halothane anesthesia, and physiologic  
 4 variables were determined 10 min and 8 h after mAb administration. Each value represents the mean ± s.e.m  
 5 of 5 rats. \*P<0.05 compared with the Pre value, #P<0.05 compared with the value at the same time point in  
 6 control IgG group. Pre, pre-ischemia.

7

1 **Supplemental Figures**

2

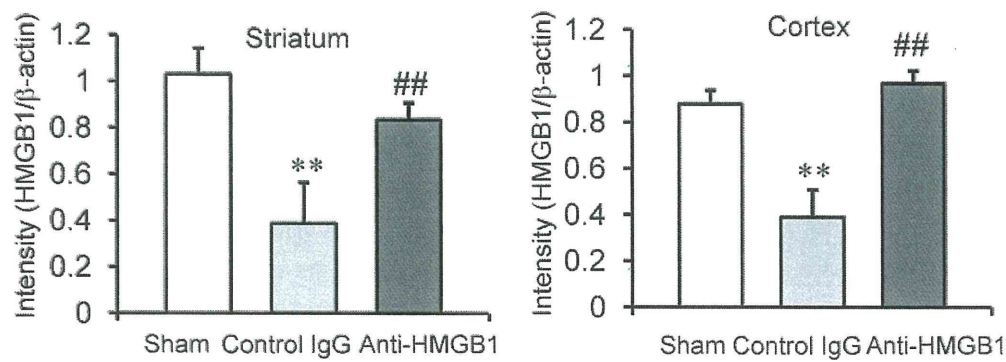
3 **A**



4

5

6 **C**



7

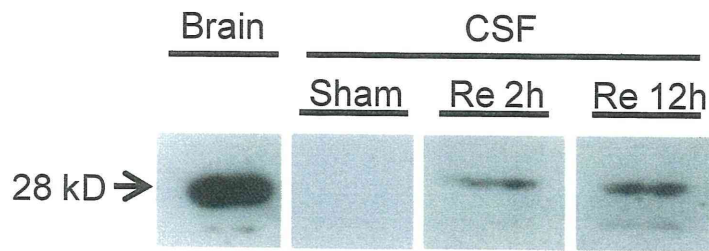
8

9 **Supplemental Figure 1**

10 Detection of HMGB1 in the ischemia core area using Western blotting. The rat brain in  
 11 control IgG-treated group and anti-HMGB1 treated group was perfused by cold saline,  
 12 collected and homogenized in RIPA solution with protease inhibitors as indicated in  
 13 supplemental methods. HMGB1 was blotted by a peroxides-labeled anti-HMGB1 mAb  
 14 (#10-22) and visualized by ECL system. β-actin was used as the internal control. (A)  
 15 The bands of HMGB1 and β-actin detected by Western blotting from 3 representative brain  
 16 samples in sham (n=5), control IgG (n=8), and anti-HMGB1 (n=8) groups. (B) A  
 17 representative image of TTC staining of a brain slice from a MCAO rat 12 h after reperfusion.  
 18 The squares circled by dash line indicate the positions where the brain samples were collected.  
 19 S: striatum, C: cortex. (C) Quantitative results of the bands detected by Western blotting  
 20 using NIH image J 1.42q software. The results are the means ± s.e.m. \*\*P<0.01 compared  
 21 with sham control, ##P<0.01 compared with control IgG group.

22

23



1

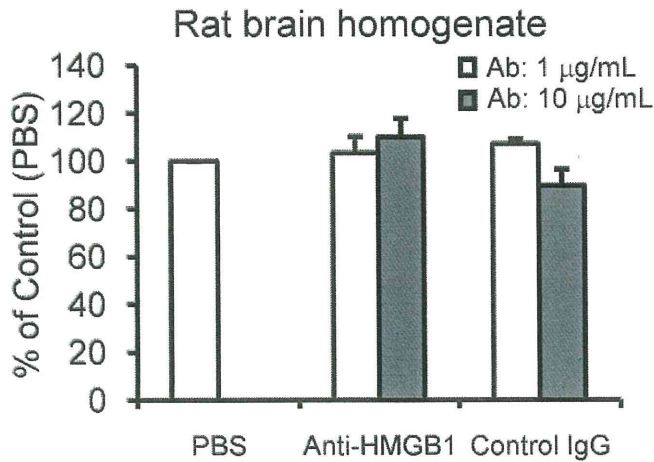
2 **Supplemental Figure 2**

3 Detection of HMGB1 in the cerebrospinal fluid after brain ischemia using Western blotting.  
 4 Cerebrospinal fluid was collected from the cisterna magna at different time points.  
 5 Homogenate sample of normal rat brain was used as the positive control. HMGB1 was  
 6 blotted by a peroxides-labeled anti-HMGB1 mAb (#10-22) and visualized by ECL system as  
 7 described in supplementary methods. (Re: reperfusion)

8

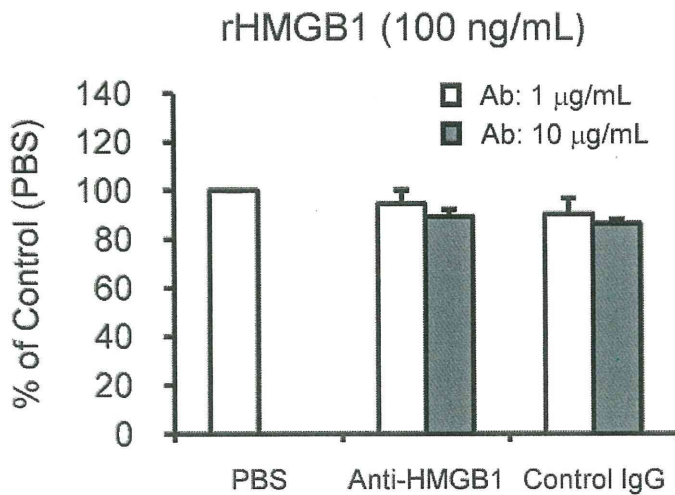
1

2 **A**



3

4 **B**



5

6 **Supplemental Figure 3**

7 Effects of anti-HMGB1 mAb (#10-22) on the ELISA. Different concentrations of  
8 anti-HMGB1 mAb were added to the incubation mixture with the brain homogenate samples  
9 containing HMGB1 (A) and rHMGB1 (B). The brain homogenizing samples were  
10 prepared by the rat brain using 50 mM Tris-HCL (pH 8.0), and diluted to 80~100 ng  
11 HMGB1 equivalent/mL by the sample buffer provided in the ELISA kit. The results are the  
12 means  $\pm$  s.e.m. of three determinations.

13